Long-range correlation in cosmic microwave background radiation

M. Sadegh Movahed,[1,2] F. Ghasemi,[3] Sohrab Rahvar,[4] and M. Reza Rahimi Tabar[4,5]
[1]*Department of Physics, Shahid Beheshti University, G.C., Evin, Tehran 19839, Iran*
[2]*School of Astronomy, Institute for Research in Fundamental Sciences, (IPM), P.O. Box 19395-5531, Tehran, Iran*
[3]*Department of Chemical Engineering & Materials Science, University of Minnesota, Minneapolis, Minnesota 55455, USA*
[4]*Department of Physics, Sharif University of Technology, P.O.Box 11365–9161, Tehran, Iran*
[5]*Fachbereich Physik, Universität Osnabrück, Barbarastraße 7, D-49076 Osnabrück, Germany*
(Received 23 March 2011; published 3 August 2011)

We investigate the statistical anisotropy and Gaussianity of temperature fluctuations of Cosmic Microwave Background (CMB) radiation data from the Wilkinson Microwave Anisotropy Probe survey, using the Multifractal Detrended Fluctuation Analysis, Rescaled Range, and Scaled Windowed Variance methods. Multifractal Detrended Fluctuation Analysis shows that CMB fluctuations has a long-range correlation function with a multifractal behavior. By comparing the shuffled and surrogate series of CMB data, we conclude that the multifractality nature of the temperature fluctuation of CMB radiation is mainly due to the long-range correlations, and the map is consistent with a Gaussian distribution.

DOI: 10.1103/PhysRevE.84.021103 PACS number(s): 05.40.−a, 05.10.Gg

I. INTRODUCTION

The Wilkinson Microwave Anisotropy Probe (WMAP) mission is designed to determine the geometry, matter content, and evolution of the universe. It has shown that the universe is geometrically flat, and dark energy at the present time has the dominant contribution in the matter content of the universe and causes the universe to have positive acceleration [1–4]. The statistical properties of the Cosmic Microwave Background (CMB) radiation data can be a unique tool to identify the parameters of standard model of cosmology [5]. One of the main aims of the statistical analysis of the CMB radiation is to examine the early universe scenarios as the inflationary cosmology. The Gaussianity of primordial fluctuations is a key assumption of modern cosmology, motivated by inflationary models [6–8].

Since the observed CMB sky is a single realization of the map of the large-scale structures, the detection of statistical isotropy violation or correlation patterns poses a great observational challenge. In order to extract more information from the rich source of information provided by present (and future) CMB maps [9–11], it is important to design as many independent statistical methods as possible to study deviations from standard statistics, such as statistical isotropy and possible correlations. Since statistical isotropy can be violated in many different ways [12], various statistical methods can come to different conclusions. Each method by design is more sensitive to a special kind of statistical isotropy violation [13–15]. Based on the bipolar power spectrum, it has shown no strong evidence of statistical isotropy violation [16–18], but analysis of the distribution of extrema in WMAP sky maps has indicated non-Gaussianity and to some extent violation of statistical isotropy [19]. In addition there are many criteria that have been introduced to measure the statistical isotropy of CMB radiation, such as quadratic maximum-likelihood [20] and multipole vectors [21], and more recently Naselsky *et al.* used symmetry of the CMB map to determine statistical isotropy as well as non-Gaussianity [22].

The statistical properties of the primordial fluctuations generated by the inflationary cosmology are closely related to the CMB radiation anisotropy, and a measurement of non-Gaussianity is a direct test of the inflation paradigm (see Refs. [23,24] for more details). Many authors have searched for non-Gaussian signatures in CMB data using peak distributions [25,26], the genus curve [27,28], peak correlations [29], global Minkowski functionals methods [30], and the directional spherical wavelet [31,32]. The techniques used for the detection of non-Gaussianity in hydrodynamic turbulence were applied for CMB data [33,34]. Moreover the Gaussianity of CMB radiation in different angular scales has been tested [35–64]. Most of the previous works tested only the consistency between the CMB data and simulated Gaussian realizations, and so far they have found no significant evidence for cosmological non-Gaussianity.

In this work we characterize the complex behavior of CMB radiation through the computation of the fluctuation parameters—scaling exponents—which quantifies the correlation exponents and multifractality of the data. We use certain fractal analysis approaches, such as Multifractal Detrended Fluctuation Analysis (MFDFA), Rescaled Range Analysis (RS), and Scaled Windowed Variance (SWV) to analyze the data set. Using the new approaches, we will test the statistical isotropy and Gaussianity of temperature fluctuations at the last scattering surface. The MFDFA method shows that CMB fluctuations have a long-range correlation function with multifractal behavior. Comparing the MFDFA results of the original temperature fluctuations to those for shuffled and surrogate series, we conclude that the multifractality nature of CMB radiation is mainly due to long-range correlations, and the map is consistent with a Gaussian distribution. Applied methods of MFDFA, RS, and SWV show that WMAP data are a statistically isotropic data set. The value of the scaling exponent (Hurst exponent) guarantees that there is no evidence for violation of statistical isotropy in the CMB anisotropy map considered here.

This paper is organized as follows: In Sec. II we briefly describe the MFDFA method and show that the scaling exponents determined via the MFDFA method are identical to those obtained by the standard multifractal formalism based on

partition functions. Also we briefly introduce the RS and SWV methods. The fractal analysis of the temperature fluctuations are presented in Sec. III. In Sec. IV, we compare the multifractal behavior of the original data with that of shuffled and surrogate series and show that the multifractality is mainly due to the long-range correlations. In Sec. V we investigate the statistical isotropy and Gaussianity of temperature fluctuations using the MFDFA, RS, and SWV results. Section VI provides discussion and presents the results.

II. FRACTAL ANALYSIS METHODS

In this section we review three standard methods: MFDFA, RS, and SWV, to investigate the fractal properties of stochastic processes.

A. Multifractal Detrended Fluctuation Analysis

The MFDFA methods are the modified version of Detrended Fluctuation Analysis (DFA) to detect multifractal properties of series. The DFA method introduced by Peng *et al.* [65] has became a widely used technique for determination of (mono)-fractal scaling properties and the detection of long-range correlations in noisy nonstationary time series [65–69]. It has successfully been applied to diverse fields such as DNA sequences [65,70], heart rate dynamics [71,72], neuron spiking [73], human gait [74], long-time weather records [75], cloud structure [76], geology [77], ethnology [78], economical time series [79], solid-state physics [80], solar physics, and plasma fluctuations [81].

The simplest type of the multifractal analysis is based upon the standard partition function multifractal formalism, which has been developed for the multifractal characterization of normalized, isotropic (stationary) measurements [82–85]. Unfortunately, this standard formalism does not give correct results for nonisotropic angular (nonstationary time) series that are affected by trends or that cannot be normalized. Thus, in the early 1990s an improved multifractal formalism was developed, the wavelet transform modulus maxima (WTMM) method [86], which is based on the wavelet analysis and involves tracing the maxima lines in the continuous wavelet transform over all scales. The other method, MFDFA, is based on the identification of scaling of the qth-order moments depending on the signal length and is a generalization of the standard DFA using only the second moment, $q = 2$.

MFDFA does not require the modulus maxima procedure in contrast to the WTMM method, and hence does not require more effort in programming and computing than the conventional DFA. On the other hand, often experimental data are affected by nonisotropic (nonstationarities) -like trends, which have to be well distinguished from the intrinsic fluctuations of the system in order to find the correct scaling behavior of the fluctuations. In addition very often we do not know the reasons for underlying trends in collected data, and even worse we do not know the scales of the underlying trends; also, usually the available recorded data is small. For the reliable detection of correlations, it is essential to distinguish trends from the intrinsic fluctuations in the data. Nondetrending methods work well if the records are long and do not involve trends. But if trends are present in the data, they might give wrong results. DFA is a well-established method for determining the scaling behavior of noisy data in the presence of trends without knowing their origin and shape [65,70,71,87,88].

The MFDFA procedure consists of five steps. The first three steps are essentially identical to the conventional DFA procedure (see, e.g., Refs, [65–69]). In our case, which is studying the temperature fluctuations of CMB radiation, we take the temperature data with the size of N and follow the steps as follows:

Step 1: Determine the "profile":

$$Y(\gamma_s) \equiv \sum_{i=1}^{s} [T(\hat{n}_i) - \langle T \rangle], \quad s = 1, \ldots, N, \tag{1}$$

where $T(\hat{n}_i)$ is the temperature of CMB map, $\hat{n_i}$ is the unit vector pointing CMB radiation, and $\gamma_s = \arccos(\hat{n}_1 . \hat{n}_s)$ is the size of the segment of CMB radiation for which we are calculating the series. Subtraction of the mean $\langle T \rangle$ is not compulsory, since it would be eliminated by the later detrending in the third step.

Step 2: Divide the profile $Y(\gamma_s)$ into $N_{\gamma_s} \equiv \text{int}(N/s)$ nonoverlapping segments of equal angular lengths γ_s.

Step 3: Calculate the local trend for each of the N_{γ_s} segments by fitting a polynomial function to $Y(\gamma_s)$. The variance between $Y(\gamma_s)$ and the function of the best fit for each segment ν, $\nu = 1, \ldots, N_{\gamma_s}$, is as follows:

$$F^2(\gamma_s, \nu) \equiv \frac{1}{s} \sum_{i=1}^{s} \{Y[(\nu - 1)\gamma_s + \gamma_i] - y_\nu(\gamma_i)\}^2 . \tag{2}$$

A linear, quadratic, cubic, or higher-order polynomial can be used in the fitting procedure (conventionally called DFA1, DFA2, DFA3, ...) [65,67,68,72].

Step 4: Average over all segments to obtain the qth-order fluctuation function, defined as

$$F_q(\gamma_s) \equiv \left\{ \frac{1}{N_{\gamma_s}} \sum_{\nu=1}^{N_{\gamma_s}} [F^2(\gamma_s, \nu)]^{q/2} \right\}^{1/q}, \tag{3}$$

where, in general, the index variable q can take any real value except zero. For $q = 0$, Eq. (3) becomes

$$F_0(\gamma_s) = \exp\left[\frac{1}{2N_{\gamma_s}} \sum_{\nu=1}^{N_{\gamma_s}} \ln F^2(\gamma_s, \nu) \right]. \tag{4}$$

For $q = 2$, the standard DFA is retrieved. Generally we are interested in how the generalized q-dependent fluctuation functions, $F_q(\gamma_s)$, depend on the angular scale γ_s for different values of q. Hence, we must repeat steps 2, 3, and 4 for several angular scales γ_s. It is apparent that $F_q(\gamma_s)$ will increase with the increasing of γ_s.

Step 5: Determine the scaling behavior of the fluctuation functions by analyzing log-log plots of $F_q(\gamma_s)$ versus γ_s for each value of q. If the series $T(\hat{n}_i)$ are long-range power-law correlated, $F_q(\gamma_s)$ increases, for large values of γ_s, as a power law:

$$F_q(\gamma_s) \sim \gamma_s^{h(q)}. \tag{5}$$

In general, the exponent $h(q)$ may depend on q. For isotropic fluctuations, $0 < h(2) < 1.0$, and $h(2)$ is identical to the well-known Hurst exponent [$h(2) = H$] [65,66,82]. In the absence of statistical isotropy the corresponding scaling exponent of $F_q(\gamma_s)$ is larger than unity $h(2) > 1.0$, and its relation to the Hurst exponent is $H = h(q = 2) - 1$ [65,81,89]. Thus, one can call the function $h(q)$ the generalized Hurst exponent.

For monofractal fluctuations, $h(q)$ is independent of q, since the scaling behavior of the variances $F^2(\gamma_s,\nu)$ is identical for all segments of ν, and the averaging procedure in Eq. (3) will just give this identical scaling behavior for all values of q. If we consider positive values of q, the segments ν with large variance $F^2(\gamma_s,\nu)$ (i.e., large deviations from the corresponding fit) will dominate the average $F_q(\gamma_s)$. Thus, for positive values of q, $h(q)$ describes the scaling behavior of the segments with large fluctuations. Usually the large fluctuations are characterized by a smaller scaling exponent $h(q)$ for multifractal series [90]. On the contrary, for negative values of q, the segments ν with small variance $F^2(\gamma_s,\nu)$ will dominate the average $F_q(\gamma_s)$. Hence, for negative values of q, $h(q)$ describes the scaling behavior of the segments with small fluctuations [90].

1. Relation to standard multifractal analysis

For an isotropic series the multifractal scaling exponents $h(q)$ defined in Eq. (5) are directly related to the scaling exponents $\tau(q)$ defined by the standard partition function-based multifractal formalism as shown below. Suppose that the data $T(\hat{n}_i)$ of length N are an isotropic sequence. Then the detrending procedure in step 3 of the MFDFA method is not required, since no trend has to be eliminated. Thus, the DFA can be replaced by the standard Fluctuation Analysis (FA) with the definition of variance for each segment ν, $\nu = 1, \ldots, N_{\gamma_s}$ as follows:

$$F^2_{\mathrm{FA}}(\gamma_s,\nu) \equiv [Y(\nu\gamma_s) - Y((\nu-1)\gamma_s)]^2. \tag{6}$$

Inserting this simplified definition into Eq. (3) and using Eq. (5), we obtain

$$\left\{ \frac{1}{N_{\gamma_s}} \sum_{\nu=1}^{N_{\gamma_s}} |Y(\nu\gamma_s) - Y((\nu-1)\gamma_s)|^q \right\}^{1/q} \sim \gamma_s^{h(q)}. \tag{7}$$

In order to relate also to the standard textbook box counting formalism [82–85], we employ the definition of the profile in Eq. (1). It is evident that the term $Y(\nu\gamma_s) - Y[(\nu-1)\gamma_s]$ in Eq. (7) is identical to the sum of the numbers $T(\hat{n}_i)$ within each segment ν of size γ_s. This sum is known as the box probability $p_{\gamma_s}(\nu)$ in the standard multifractal formalism for $T(\hat{n}_i)$:

$$p_{\gamma_s}(\nu) \equiv \sum_{i=(\nu-1)s+1}^{\nu s} T(n_i) = Y(\nu\gamma_s) - Y[(\nu-1)\gamma_s]. \tag{8}$$

The scaling exponent $\tau(q)$ is usually defined via the partition function $Z_q(\gamma_s)$:

$$Z_q(\gamma_s) \equiv \sum_{\nu=1}^{N_{\gamma_s}} |p_{\gamma_s}(\nu)|^q \sim \gamma_s^{\tau(q)}, \tag{9}$$

where q is a real parameter as in the MFDFA method, discussed above. Using Eq. (8), we see that Eq. (9) is identical to Eq. (7), and obtain analytically the relation between the two sets of multifractal scaling exponents:

$$\tau(q) = qh(q) - 1. \tag{10}$$

Thus, we observe that $h(q)$ defined in Eq. (5) for the MFDFA is directly related to the classical multifractal scaling exponents $\tau(q)$. Note that $h(q)$ is different from the generalized multifractal dimensions, defined as

$$D(q) \equiv \frac{\tau(q)}{q-1}, \tag{11}$$

which are used instead of $\tau(q)$ in some papers. While $h(q)$ is independent of q for a monofractal time series, $D(q)$ depends on q in this case. Another way to characterize a multifractal series is the singularity spectrum $f(\alpha)$, which is related to $\tau(q)$ via a Legendre transform [82,84]:

$$\alpha = \tau'(q) \quad \text{and} \quad f(\alpha) = q\alpha - \tau(q). \tag{12}$$

Here α is the singularity strength or Hölder exponent, while $f(\alpha)$ denotes the dimension of the subset of the series that is characterized by α. Using Eq. (10), we can directly relate α and $f(\alpha)$ to $h(q)$:

$$\alpha = h(q) + qh'(q) \quad \text{and} \quad f(\alpha) = q[\alpha - h(q)] + 1. \tag{13}$$

A Hölder exponent denotes monofractality, while in the multifractal case, the different parts of the structure are characterized by different values of α, leading to the existence of the spectrum $f(\alpha)$. The interval of Hölder spectrum for a multifractal process, $\alpha \in [\alpha_{\min},\alpha_{\max}]$, can be determined by [91]

$$\alpha_{\min} = \lim_{q\to+\infty} \frac{\partial\tau(q)}{\partial q}, \tag{14}$$

$$\alpha_{\max} = \lim_{q\to-\infty} \frac{\partial\tau(q)}{\partial q} \tag{15}$$

B. Scaled Windowed Variance Analysis

Scaled Windowed Variance (SWV) analysis was developed by Cannon *et al.* [89]. The profile of temperature $Y(\gamma_s)$ is divided into intervals of angular length scale γ_s. Then the standard deviation is calculated within each interval using the following relation:

$$\mathrm{SWV}(\gamma_s) = \left\{ \frac{1}{s} \sum_{i=1}^{s} [Y(\gamma_i) - \langle Y(\gamma_s)\rangle]^2 \right\}^{1/2}. \tag{16}$$

The average standard deviation of all angular intervals of length γ_s is computed. This computation is repeated over all possible interval lengths. The SWV is related to γ_s by a power law:

$$\mathrm{SWV} \sim \gamma_s^H. \tag{17}$$

C. Rescaled Range Analysis

Hurst developed RS, a statistical method to analyze long records of natural phenomena [89,92]. There are two factors

used in this analysis: first, the range R, which is the difference between the minimum and maximum "accumulated" values or cumulative sum of $X(t,\tau)$ of a typical natural phenomenon at discrete time t over a time span τ, and second, the standard deviation S, estimated from the observed values $X(t,\tau)$. Hurst found that the ratio RS is very well described for a large number of natural phenomena by the following empirical relation:

$$\mathrm{RS} \sim \tau^H, \tag{18}$$

where τ and H are time span and Hurst exponent, respectively. For temperature fluctuations on the last scattering surface, R and S are defined as

$$R(\gamma_s) = \mathrm{Max}[Y(\gamma_s)] - \mathrm{Min}[Y(\gamma_s)], \tag{19}$$

$$S(\gamma_s) = \left\{ \frac{1}{s} \sum_{i=1}^{s} [T(\hat{n}_i) - \langle T \rangle]^2 \right\}^{1/2}, \quad s = 1, \ldots, N, \tag{20}$$

where $Y(\gamma_s)$ is defined according to Eq. (1). The scaling behavior of the fluctuation function is determined by analyzing log-log plot of RS versus γ_s as

$$\mathrm{RS} \sim \gamma_s^H. \tag{21}$$

III. FRACTAL ANALYSIS OF COSMIC MICROWAVE BACKGROUND RADIATION DATA

As mentioned in Sec. II, a spurious of correlations may be detected in the absence of statistical isotropy, so direct calculation of correlation functions, fractal dimensions etc., may not give reliable results [65,66,82,89,90]. The simplest way to verify the statistical isotropy of the temperature fluctuations on the last scattering surface is by measuring the stability of the variance of the temperature in various sizes of windows. Figure 1 shows the standard deviation of the temperature verses the angular size γ_s of the window. Here we have a saturation for the standard derivation in the large angular

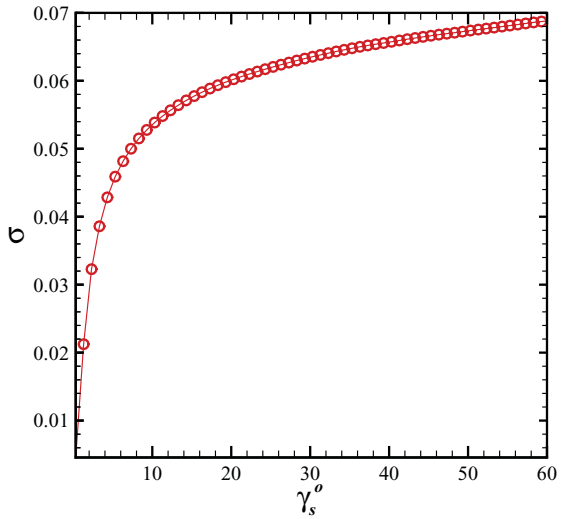

FIG. 1. (Color online) Behavior of standard deviation of temperature fluctuations of CMB radiation as a function of angular scale γ_s.

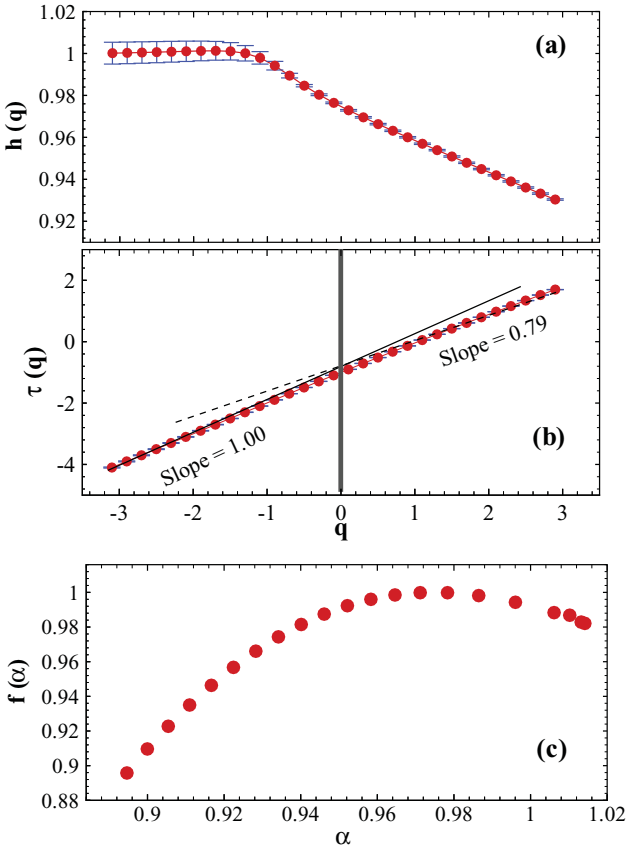

FIG. 2. (Color online) The q dependence of the generalized Hurst exponent $h(q)$, the corresponding $\tau(q)$, and singularity spectrum $f(\alpha)$ are shown in the upper to lower panels, respectively, for temperature fluctuation series.

scale, which reflects the long-range correlation behavior of the temperature fluctuations of CMB radiation [65,66,82,89,90].

We use the MFDFA1 method for analyzing the temperature fluctuations in CMB radiation. Following the procedure for MFDFA analysis as described in the last section we obtain $F_q(\gamma_s)$ as a function of angular scale γ_s. For each index of q the generalized Hurst exponents, $h(q)$ in Eq. (5) can be found by analyzing log-log plots of $F_q(\gamma_s)$ versus γ_s. Figure 2 shows the Hurst exponent in terms of q for MFDFA1 analysis. Variation of the Hurst exponent in terms of q shows the multifractal behavior of temperature fluctuation of the CMB radiation. Moreover we have different values of the slope of classical multifractal scaling exponent $\tau(q)$ for $q < 0$ and $q > 0$, which indicates that CMB radiation has a multifractal structure. For positive and negative values of q, we obtain $\tau(q)$ with slopes 0.79 ± 0.03 and 1.00 ± 0.03, respectively, at a 1σ confidence interval. According to the relation between the Hurst exponent and MFDFA exponent, we obtain $H = 0.94 \pm 0.01$ at a 1σ confidence interval, which means that temperature fluctuation is an isotropic process with long-range correlation [90]. The variation of singularity spectrum $f(\alpha)$ [Eq. (12)] also is shown in Fig. 2. The values of derived quantities from the MFDFA1 method are given in Table I.

We also use SWV analysis [89,92] to determine the Hurst exponent for CMB radiation via Eq. (17). Figure 3 shows log-log plot of SWV of CMB fluctuations as a function of

TABLE I. The values of the Hurst, multifractal scaling, and generalized multifractal exponents for $q = 2.0$ at a 1σ confidence interval, for original, surrogate, and shuffled temperature fluctuation series obtained by MFDFA1.

Data	H	τ	D
CMB	0.94 ± 0.01	0.88 ± 0.02	0.88 ± 0.02
Surrogate	0.88 ± 0.01	0.76 ± 0.02	0.76 ± 0.02
Shuffled	0.500 ± 0.001	0.002 ± 0.002	0.002 ± 0.002

angular scale γ_s, which results in $H = 0.95 \pm 0.02$ at a 68% confidence interval. Finally we apply RS to determine the Hurst exponent of CMB fluctuations. According to Fig. 4, the value of the Hurst exponent obtained is 0.95 ± 0.02 at a 68% confidence interval, which is in agreement with the two previous results.

IV. COMPARISON OF MULTIFRACTAL NATURE FOR ORIGINAL, SHUFFLED, AND SURROGATE CMB DATA

In this section we are interested in determining the source of multifractality and testing the Gaussianity of CMB data. In general, two different types of multifractality in certain data sets can be distinguished: (1) multifractality due to a fatness of the probability density function (PDF) and (2) multifractality due to different correlations in small- and large-scale fluctuations. In the first case the multifractality cannot be removed by shuffling the data set, while in the second case data may have a PDF with finite moments; e.g., a Gaussian distribution and the corresponding shuffled series will exhibit monofractal scaling, since all long-range correlations are destroyed by the shuffling procedure.

If we have both kinds of multifractality in data, the shuffled series will show weaker multifractality than the original series. The easiest way to distinguish the type of multifractality is by analyzing the corresponding shuffled and surrogate series. The shuffling of the data set destroys the long-range

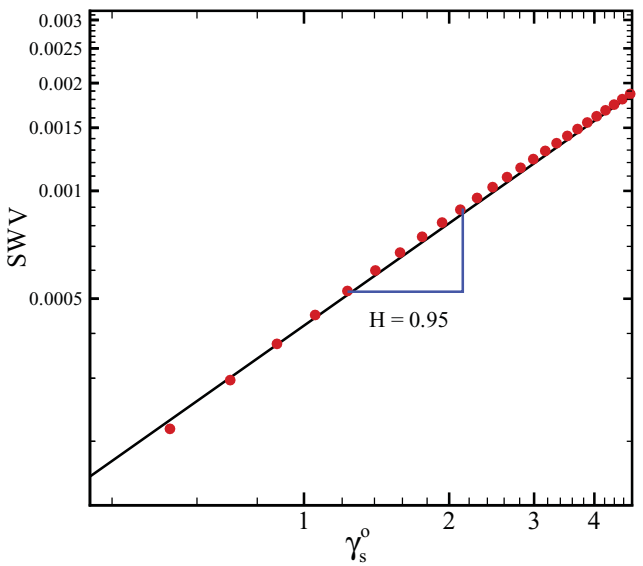

FIG. 3. (Color online) Behavior of SWV of CMB fluctuations as a function of angular scale γ_s in log-log plot.

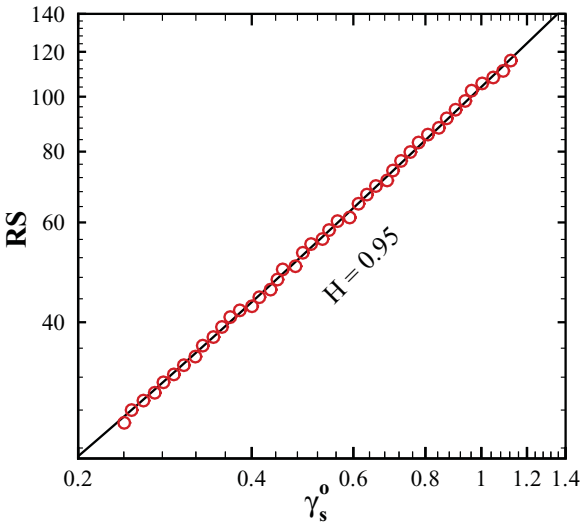

FIG. 4. (Color online) The log-log plot of RS vs angular scale γ_s for temperature fluctuation at the last scattering surface.

correlation; therefore if the multifractality belongs only to the long-range correlation, we should find $h_{\rm shuf}(q) = 0.5$ [90]. The multifractality nature due to the fatness of the PDF signals is not affected by the shuffling procedure. On the other hand, to determine the multifractality due to the broadness of PDF by the surrogating method, the phase of discrete Fourier transform (DFT) coefficients of CMB data is replaced with a set of pseudo-independent uniform distribution within the range of $(-\pi,\pi)$ [81,93]. The correlations in the surrogate series do not change, while the probability function changes to the Gaussian distribution. If multifractality in the data set is due to a broadness of PDF, $h(q)$ obtained by the surrogate method will be independent of q. If both kinds of multifractality are present in CMB data, the shuffled and surrogate series will show weaker multifractality than the original one.

To check the nature of multifractality, we compare the fluctuation function $F_q(\gamma_s)$, for the CMB map with the result of the corresponding shuffled $F_q^{\rm shuf}(\gamma_s)$ and surrogate $F_q^{\rm sur}(\gamma_s)$ data. Differences between these two fluctuation functions and the original one can indicate the presence of long-range correlations or broadness of the probability density function in the original data. These differences can be obtained by the ratio $F_q(\gamma_s)/F_q^{\rm shuf}(\gamma_s)$ and $F_q(\gamma_s)/F_q^{\rm sur}(\gamma_s)$ as a function of γ_s [90]. Since the anomalous scaling due to a broad probability density affects $F_q(\gamma_s)$ and $F_q^{\rm shuf}(\gamma_s)$ in the same way, only multifractality due to correlations will be observed in $F_q(\gamma_s)/F_q^{\rm shuf}(\gamma_s)$. The scaling behavior of these ratios is

$$F_q(\gamma_s)/F_q^{\rm shuf}(\gamma_s) \sim \gamma_s^{h(q)-h_{\rm shuf}(q)} = \gamma_s^{h_{\rm corr}(q)}, \quad (22)$$

$$F_q(\gamma_s)/F_q^{\rm sur}(\gamma_s) \sim \gamma_s^{h(q)-h_{\rm sur}(q)} = \gamma_s^{h_{\rm PDF}(q)}. \quad (23)$$

If only fatness of the PDF is responsible for the multifractality, one should find $h(q) = h_{\rm shuf}(q)$ and $h_{\rm corr}(q) = 0$. On the other hand, deviations from $h_{\rm corr}(q) = 0$ indicate the presence of correlations, and q dependence of $h_{\rm corr}(q)$ indicates that multifractality is due to the long-range correlation.

If the multifractal behavior of CMB is made by the broadness of PDF and long-range correlation, both $h_{\rm shuf}(q)$

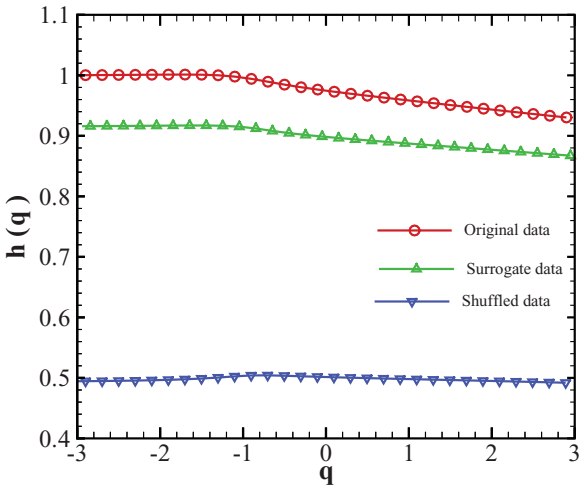

FIG. 5. (Color online) Generalized Hurst exponent as a function of q for original, surrogate, and shuffled CMB data.

and $h_{\rm sur}(q)$ will depend on q. The q dependence of the generalized exponent $h(q)$ for original, surrogate, and shuffled CMB data is shown in Fig. 5, which shows that the multifractality nature of temperature fluctuation is almost due to the *long-range* correlation. The absolute value of $h_{\rm corr}(q)$ is larger than $h_{\rm PDF}(q)$, which indicates that the multifractality due to the fatness is much weaker than the multifractality due to the correlation. The deviation of $h_{\rm sur}(q)$ and $h_{\rm shuf}(q)$ from $h(q)$ can be determined by using χ^2 as follows:

$$\chi^2_{\diamond} = \sum_{i=1}^{N} \frac{[h(q_i) - h_{\diamond}(q_i)]^2}{\sigma(q_i)^2 + \sigma_{\diamond}(q_i)^2}, \tag{24}$$

where the symbol "$\diamond$" represents for "surrogate" or "shuffled" series. The value of reduced chi-square $\chi^2_{\nu\diamond} = \chi^2_{\diamond}/\mathcal{N}$ ($\mathcal{N}$ is the number of degrees of freedom) for shuffled and surrogate time series is 21 599 and 313, respectively.

The singularity spectrum $f(\alpha)$ of the surrogate series is almost similar to the original temperature fluctuations, while in the case of shuffled series we have a narrower singularity spectrum of $\Delta\alpha_{\rm shuf} = \alpha(q_{\rm min}) - \alpha(q_{\rm max}) \simeq 0.02$ compared to that of surrogate $\Delta\alpha_{\rm sur} \simeq 0.09$ and original data $\Delta\alpha \simeq 0.12$. The small value of $\Delta\alpha_{\rm shuf}$ compared to the two other series shows that the multifractality in the shuffled CMB map has almost been destroyed [94]. Figures 6 and 7 show the MFDFA1 results for surrogate and shuffled temperature fluctuation series. Comparing the MFDFA results of the data set to those for shuffled and surrogate series, we conclude that the multifractal nature of temperature fluctuations in CMB data is almost due to the *long-range correlations*, and the probability distribution function of CMB is almost Gaussian (see also Sec. V). The values of the Hurst exponent H, multifractal scaling $\tau(q = 2)$, and generalized multifractal dimension $D(q = 2)$ of the original, shuffled, and surrogate data of CMB obtained with the MFDFA1 method are reported in Table I.

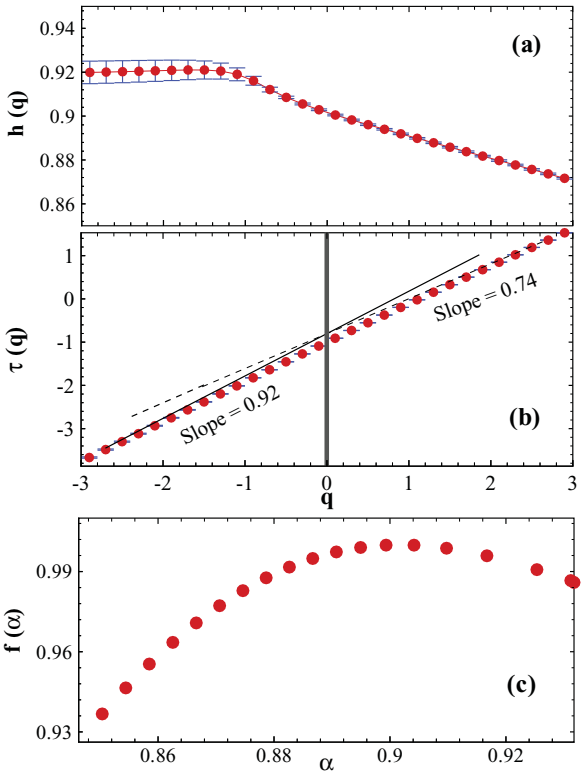

FIG. 6. (Color online) The q dependence of the generalized Hurst exponent $h(q)$, the corresponding $\tau(q)$, and singularity spectrum $f(\alpha)$ are shown in the upper to lower panels, respectively, for surrogate temperature fluctuation series.

V. STATISTICAL ISOTROPY AND GAUSSIANITY OF CMB ANISOTROPY

In this section we examine the Gaussianity and statistical isotropy of temperature fluctuations in CMB data through MFDFA, RS, and SWV methods.

Standard models of inflationary cosmology predict a Gaussian distribution of CMB temperature fluctuations. However, along with standard inflationary models, there exist theories such as inflationary scenarios with two or more scalar fields that predict a non-Gaussian primordial fluctuations [95–101]. Another possibility of deviation from Gaussianity is the manipulation of the CMB signals after the recombination due to subsequent weak gravitational lensing [102,103] and various foregrounds like dust emission, synchrotron radiation, or unresolved point sources [104]. One should also take into account the additional instrumental noise in the observational data [105]. One of the advantages of Gaussian field is that the two-point correlation function $C(\hat{n}, \hat{n}') \equiv \langle T(\hat{n})T(\hat{n}')\rangle$ will be sufficient to fully specify the statistical properties of the field. In the case of non-Gaussianity, one must take the higher moments of the field into account in order to fully describe the whole statistics. So, studying the Gaussian nature of the signals or detecting some distinctive non-Gaussianity is an important issue to understand the statistical properties of CMB radiation.

As we have seen in Sec. IV, the MFDFA1 results of the shuffled series show almost constant $h(q) \simeq 0.5$, which

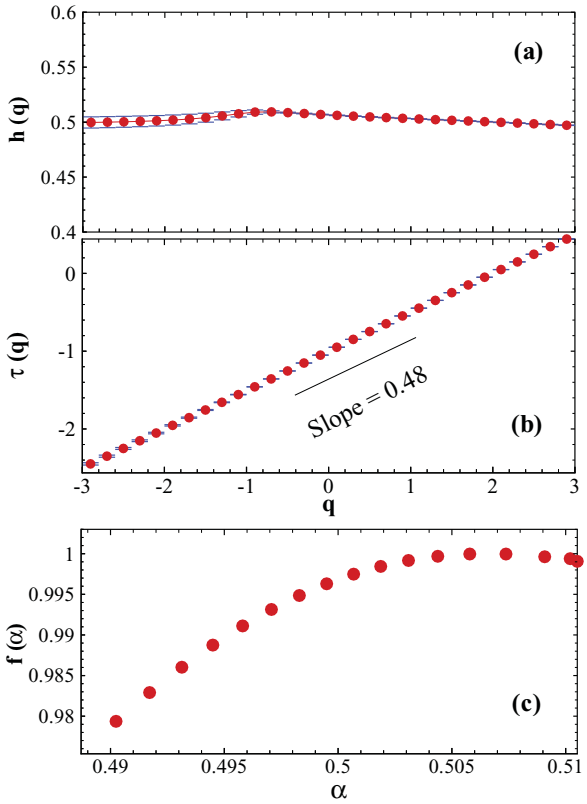

FIG. 7. (Color online) The q dependence of the generalized Hurst exponent $h(q)$, corresponding $\tau(q)$, and singularity spectrum $f(\alpha)$ are shown in the upper to lower panels, respectively, for shuffled temperature fluctuation series.

indicates that $h(q)$ is independent of the q, or in other words the shuffled series is a monofractal structure. This means that the multifractality of the original data is due to the long-range correlations, not due to a broadness of PDF of temperature fluctuations (Fig. 5). Furthermore small differences in the generalized Hurst exponent between the original and surrogated data (Fig. 5) and similarity of the singularity spectrum $f(\alpha)$ in those two series show that the probability density function of temperature fluctuations has good confidence with the Gaussian distribution, which is in agreement with the recent results [16,17,33,34].

The second important question about the CMB data is its statistical isotropy. One of the main motivations for anisotropy of the universe comes from the global topology of the universe. The idea of a multiconnected topology of the universe comes back to Schwarzschild's work [106] before Einstein's first seminal paper on cosmology [107]. If the universe is assumed to be simply connected, the cosmological principle implies that it should be globally isotropic to any observer. In the case of a multiconnected universe, while the Einstein gravity still holds in this space, the global structure of universe at large scales will be more complicated. One of the most promising signatures may be in the CMB radiation as the existence of large-scale anisotropies with a repeating pattern [108]. In addition to cosmological mechanisms, instrumental and environmental effects in observations of CMB radiation can also easily produce a spurious breakdown of statistical isotropy. Here we examine the anisotropy of CMB radiation with the MFDFA analysis.

The statistical isotropy means that the statistical properties of CMB radiation (e.g., n-point correlations) are invariant under Eulerian rotation. This means that the two-point correlation function is a function of an angle between two points:

$$C(\hat{n}_1,\hat{n}_2) = C(\hat{n}_1 \cdot \hat{n}_2) \equiv C(\gamma), \tag{25}$$

where $\gamma = \arccos(\hat{n}_1 \cdot \hat{n}_2)$ is the angle between $\hat{n}_1$ and $\hat{n}_2$. It is then convenient to expand it in terms of Legendre polynomials:

$$C(\gamma) = \frac{1}{4\pi}\sum_{l=2}^{\infty}(2l+1)C_l P_l(\cos\gamma), \tag{26}$$

where C_l is the widely used *angular power spectrum*. The summation over l starts from 2 because the $l = 0$ term is the monopole where in the case of statistical isotropy the monopole is constant, and it can be subtracted out. The dipole $l = 1$ is due to the local motion of the observer with respect to the last scattering surface and can be subtracted out as well. In order to extract the statistical property of CMB radiation we need an ensemble map from it to calculate the correlation functions. In reality we have only one map from the CMB, but if we assume the statistical isotropy ,we can calculate the correlation functions moving in overall data. As we mentioned in Sec. II, for a process with stationarity in time or an isotropic process in space, the Hurst exponent is always less than unity [65,89]. According to the MF-DAF1, SWV, and RS methods we obtained the value of the Hurst exponent for WMAP data as $H = 0.94 \pm 0.02$ at a 1σ confidence interval. These analyses with the Hurst exponent $(0 < H < 1.0)$ show that there is no evidence for violation of statistical isotropy of WMAP data.

VI. CONCLUSION

In this work we used three methods to investigate the statistical properties of WMAP data. Multifractal Detrended Fluctuation Analysis, Rescaled Range Analysis, and Scaled Windowed Variance methods show that the WMAP data are a statistically isotropic data set. The value of the Hurst exponent, $H \simeq 0.94$, guarantees that there is no evidence for violation of statistical isotropy in the CMB map. The MFDFA method allows us to determine the multifractal characterization of this map. The q dependence of generalized Hurst $h(q)$ and classical multifractal scaling $\tau(q)$ exponents shows that the temperature fluctuations on the last scattering surface have a multifractal behavior [33]. We obtained the generalized multifractal dimension of CMB data, $D \simeq 0.88$. According to a small difference between the generalized Hurst exponent and the singularity spectrum of the original data set with the surrogate ones, $H - H_{\rm sur} = 0.06 \pm 0.01$ and $\Delta\alpha - \Delta\alpha_{\rm sur} = 0.03$, we found that there is no crucial evidence for non-Gaussianity of the CMB map. The compatibility of the multifractal behavior of the temperature fluctuations of CMB radiation with their Gaussian distribution has been also explored recently [109]. Comparison of the generalized Hurst

exponent of the original data with the shuffled and surrogate series showed that the nature of the multifractality of CMB is mainly due to the long-range correlation, rather than the broadness of the probability density function.

ACKNOWLEDGMENTS

We would like to thank M. Fazeli and G. R. Jafari for useful discussions.

[1] N. Afshordi, Y. Loh, and M. A. Strauss, Phys. Rev. D **69**, 083524 (2004).
[2] C. L. Bennett *et al.*, Astrophys. J. Suppl. Ser. **148**, 213 (2003).
[3] D. N. Spergel *et al.*, Astrophys. J. Suppl. Ser. **148**, 175 (2003).
[4] M. Tegmark *et al.*, Phys. Rev. D **69**, 103501 (2004).
[5] H. V. Peiris *et al.*, Astrophys. J. Supp. Ser. **148**, 213 (2003).
[6] V. F. Mukhanov and G. V. Chibisov, J. Exp. Theor. Phys. Lett. **33**, 532 (1981).
[7] S. W. Hawking, Phys. Lett. B **115**, 295 (1982).
[8] A. H. Guth and S. Y. Pi, Phys. Rev. Lett. **49**, 1110 (1982).
[9] Planck Collaboration, e-print arXiv:1101.2028.
[10] Planck Collaboration, e-print arXiv:1101.2022.
[11] E. Shirokoff *et al.*, Astrophys. J. **736**, 61 (2011).
[12] L. Ackerman, S. M. Carroll, and M. B. Wise, Phys. Rev. D **75**, 083502 (2007).
[13] Z. Hou, A. J. Banday, K. M. Gorski, N. E. Groeneboom, and H. K. Eriksen, Mon. Not. R. Astron. Soc. **401**, 2379 (2010).
[14] N. Joshi, S. Jhingan, T. Souradeep, and A. Hajian, Phys. Rev. D **81**, 083012 (2010).
[15] M. Aich and T. Souradeep, Phys. Rev. D **81**, 083008 (2010).
[16] T. Souradeep, A. Hajian, and S. Basak, New Astron. Rev. **50**, 889 (2006).
[17] A. Hajian, T. Souradeep, and N. Cornish, Astrophys. J. **618**, L63 (2005).
[18] A. Hajian and T. Souradeep, Phys. Rev. D **74**, 123521 (2006).
[19] D. L. Larson and B. D. Wandelt, Astrophys. J. **613**, L85 (2004).
[20] D. Hanson and A. Lewis, Phys. Rev. D **80**, 063004 (2009).
[21] C. Zunckel, D. Huterer, and G. D. Starkman, e-print arXiv:1009.4701.
[22] P. Naselsky, M. Hansen, and J. Kim, e-print arXiv:1105.4426.
[23] N. Bartolo, S. Matarrese, and A. Riotto, Adv. Astron. (2010), id. 157079, e-print arXiv:1001.3957.
[24] L. R. Abramo and T. S. Pereira, Adv. Astron. **2010**, 378203 (2010).
[25] J. M. Bardeen, J. R. Bond, N. Kaiser, and A. S. Szalay, Astrophys. J. **304**, 15 (1986).
[26] J. R. Bond and G. Efstathiou, Mon. Not. R. Astron. Soc. **226**, 655 (1987).
[27] P. Coles, Mon. Not. R. Astron. Soc. **234**, 509 (1988).
[28] G. F. Smoot, L. Tenorio, A. J. Banday, A. Kogut, E. L. Wright, G. Hinshaw, and C. L. Bennett, Astrophys. J. **437**, 1 (1994).
[29] A. Kogut, A. J. Banday, C. L. Bennett, K. M. Gorski, G. Hinshaw, G. F. Smoot, and E. L. Wright, Astrophys. J. Lett. **464**, L29 (1996).
[30] S. Winitzki and A. Kosowsky, New Astron. Rev. **3**, 75 (1998).
[31] J. D. McEwen, M. P. Hobson, A. N. Lasenby, and D. J. Mortlock, Mon. Not. R. Astron. Soc. **388**, 659 (2008).
[32] J. D. McEwen, M. P. Hobson, A. N. Lasenby, and D. J. Mortlock, Mon. Not. R. Astron. Soc. **371**, L50 (2006).
[33] A. Bershadskii and K. R. Sreenivasan, Phys. Lett. A. **319**, 21 (2003).
[34] F. Ghasemi, A. Bahraminasab, M. S. Movahed, Sohrab Rahvar, K. R. Sreenivasan, and M. Reza Rahimi Tabar, J. Stat. Mech. (2006) P11008.
[35] A. F. Heavens, Mon. Not. R. Astron. Soc. **299**, 805 (1998).
[36] J. A. Peacock and A. F. Heavens, Mon. Not. R. Astron. Soc. **217**, 805 (1985).
[37] A. F. Heavens and R. K. Sheth, Mon. Not. R. Astron. Soc. **310**, 1062 (1999).
[38] A. F. Heavens and S. Gupta, Mon. Not. R. Astron. Soc. **324**, 960 (2001).
[39] J. Schmalzing and K. M. Gorski, Mon. Not. R. Astron. Soc. **297**, 355 (1998).
[40] P. G. Ferreira, J. Magueijo, and K. M. Górski, Astrophys. J. Lett. **503**, L1 (1998).
[41] J. Pando, D. Valls-Gabaud, and L. Z. Fang, Phys. Rev. Lett. **81**, 4568 (1998).
[42] B. C. Bromley and M. Tegmark, Astrophys. J. Lett. **524**, L79 (1999).
[43] A. J. Banday, S. Zaroubi, and K. M. Górski, Astrophys. J. **533**, 575 (2000).
[44] C. R. Contaldi, P. G. Ferreira, J. Magueijo, and K. M. Górski, Astrophys. J. **534**, 25 (2000).
[45] P. Mukherjee, M. P. Hobson, and A. N. Lasenby, Mon. Not. R. Astron. Soc. **318**, 1157 (2000).
[46] J. Magueijo, Astrophys. J. Lett. **528**, L57 (2000).
[47] D. Novikov, J. Schmalzing, and V. F. Mukhanov, Astron. Astrophys. **364**, 17 (2000).
[48] H. B. Sandvik and J. Magueijo, Mon. Not. R. Astron. Soc. **325**, 463 (2001).
[49] R. B. Barreiro, M. P. Hobson, A. N. Lasenby, A. J. Banday, K. M. Górski, and G. Hinshaw, Mon. Not. R. Astron. Soc. **318**, 475 (2000).
[50] N. G. Phillips and A. Kogut, Astrophys. J. **548**, 540 (2001).
[51] E. Komatsu and U. Seljak, Mon. Not. R. Astron. Soc. **336**, 1256 (2002).
[52] E. Komatsu and D. N. Spergel, Phys. Rev. D **63**, 63002 (2001).
[53] M. Kunz, A. J. Banday, P. G. Castro, P. G. Ferreira, and K. M. Górski, Astrophys. J. Lett. **563**, L99 (2001).
[54] N. Aghanim, O. Forni, and F. R. Bouchet, Astron. Astrophys. **365**, 341 (2001).
[55] L. Cayón, E. Martinez-Gonzalez, F. Argueso, A. J. Banday, and K. M. Górski, Mon. Not. R. Astron. Soc. **339**, 1189 (2003).
[56] C. Park, B. Ratra, and M. Tegmark, Astrophys. J. **556**, 582 (2001).
[57] S. F. Shandarin, H. A. Feldman, Y. Xu, and M. Tegmark, Astrophys. J. Supp. **141**, 1 (2002).

[58] J. H. Wu *et al.*, Phys. Rev. Lett. **87**, 251303 (2001).
[59] M. G. Santos, A. Cooray, Z. Haiman, L. Knox, and C. Ma, Astrophys. J. **598**, 756 (2003).
[60] G. Polenta *et al.*, Astrophys. J. Lett. **572**, L27 (2002).
[61] J. M. G. Mead, A. Lewis, and L. King, Phys. Rev. D **83**, 023507 (2011).
[62] B. Lew, J. Cosmol. Astropart. Phys. 08 (2008) 017.
[63] C. Raeth, G. Rossmanith, G. Morfill, A. J. Banday, and K. M. Gorski, e-print arXiv:1005.2481.
[64] D. Huterer, E. Komatsu, and S. Shandera, e-print arXiv:1012.3744.
[65] C. K. Peng, S. V. Buldyrev, S. Havlin, M. Simons, H. E. Stanley, and A. L. Goldberger, Phys. Rev. E **49**, 1685 (1994); S. M. Ossadnik, S. B. Buldyrev, A. L. Goldberger, S. Havlin, R. N. Mantegna, C.-K. Peng, M. Simons, and H. E. Stanley, Biophys. J. **67**, 64 (1994).
[66] M. S. Taqqu, V. Teverovsky, and W. Willinger, Fractals **3**, 785 (1995).
[67] J. W. Kantelhardt, E. Koscielny-Bunde, H. H. A. Rego, S. Havlin, and A. Bunde, Physica A **295**, 441 (2001).
[68] K. Hu, P. C. Ivanov, Z. Chen, P. Carpena, and H. E. Stanley, Phys. Rev. E **64**, 011114 (2001).
[69] Z. Chen, P. C. Ivanov, K. Hu, and H. E. Stanley, Phys. Rev. E **65**, 041107 (2002).
[70] S. V. Buldyrev, A. L. Goldberger, S. Havlin, R. N. Mantegna, M. E. Matsa, C. K. Peng, M. Simons, and H. E. Stanley, Phys. Rev. E **51**, 5084 (1995); S. V. Buldyrev, N. V. Dokholyan, A. L. Goldberger, S. Havlin, C. K. Peng, H. E. Stanley, and G. M. Viswanathan, Physica A **249**, 430 (1998).
[71] C. K. Peng, S. Havlin, H. E. Stanley, and A. L. Goldberger, Chaos **5**, 82 (1995); P. C. Ivanov, A. Bunde, L. A. N. Amaral, S. Havlin, J. Fritsch-Yelle, R. M. Baevsky, H. E. Stanley, and A. L. Goldberger, Europhys. Lett. **48**, 594 (1999); Y. Ashkenazy, M. Lewkowicz, J. Levitan, S. Havlin, K. Saermark, H. Moelgaard, P. E. B. Thomsen, M. Moller, U. Hintze, and H. V. Huikuri, *ibid.* **53**, 709 (2001); Y. Ashkenazy, P. C. Ivanov, S. Havlin, C. K. Peng, A. L. Goldberger, and H. E. Stanley, Phys. Rev. Lett. **86**, 1900 (2001).
[72] A. Bunde, S. Havlin, J. W. Kantelhardt, T. Penzel, J.-H. Peter, and K. Voigt, Phys. Rev. Lett. **85**, 3736 (2000).
[73] S. Blesic, S. Milosevic, D. Stratimirovic, and M. Ljubisavljevic, Physica A **268**, 275 (1999); S. Bahar, J. W. Kantelhardt, A. Neiman, H. H. A. Rego, D. F. Russell, L. Wilkens, A. Bunde, and F. Moss, Europhys. Lett. **56**, 454 (2001).
[74] J. M. Hausdorff, S. L. Mitchell, R. Firtion, C. K. Peng, M. E. Cudkowicz, J. Y. Wei, and A. L. Goldberger, J. Appl. Phys. **82**, 262 (1997).
[75] E. Koscielny-Bunde, A. Bunde, S. Havlin, H. E. Roman, Y. Goldreich, and H. J. Schellnhuber, Phys. Rev. Lett. **81**, 729 (1998); K. Ivanova and M. Ausloos, Physica A **274**, 349 (1999); P. Talkner and R. O. Weber, Phys. Rev. E **62**, 150 (2000); R. G. Kavasseri and R. Nagarajian, IEEE Trans. Circuit Syst. **51**, 2255 (2004).
[76] K. Ivanova, M. Ausloos, E. E. Clothiaux, and T. P. Ackerman, Europhys. Lett. **52**, 40 (2000).
[77] B. D. Malamud and D. L. Turcotte, J. Stat. Plan. Infer. **80**, 173 (1999).
[78] C. L. Alados and M. A. Huffman, Ethnology **106**, 105 (2000).
[79] R. N. Mantegna and H. E. Stanley, *An Introduction to Econophysics* (Cambridge University Press, Cambridge, 2000); Y. Liu, P. Gopikrishnan, P. Cizeau, M. Meyer, C. K. Peng, and H. E. Stanley, Phys. Rev. E **60**, 1390 (1999); N. Vandewalle, M. Ausloos, and P. Boveroux, Physica A **269**, 170 (1999); P. Oswiecimka, J. Kwapien, and S. Drozdz, *ibid.* **347**, 626 (2005).
[80] J. W. Kantelhardt, R. Berkovits, S. Havlin, and A. Bunde, Physica A **266**, 461 (1999); N. Vandewalle, M. Ausloos, M. Houssa, P. W. Mertens, and M. M. Heyns, Appl. Phys. Lett. **74**, 1579 (1999).
[81] M. Sadegh Movahed, G. R. Jafari, F. Ghasemi, Sohrab Rahvar, and M. Reza Rahimi Tabar, J. Stat. Mech. (2006) P02003; S. Kimiagar, M. S. Movahed, S. Khorram, S. Sobhanian, and M. Reza Rahimi Tabar, *ibid.* (2009) P03020.
[82] J. Feder, *Fractals* (Plenum Press, New York, 1988).
[83] A. L. Barabási and T. Vicsek, Phys. Rev. A **44**, 2730 (1991).
[84] H. O. Peitgen, H. Jürgens, and D. Saupe, *Chaos and Fractals* (Springer, New York, 1992), Appendix B.
[85] E. Bacry, J. Delour, and J. F. Muzy, Phys. Rev. E **64**, 026103 (2001).
[86] J. F. Muzy, E. Bacry, and A. Arneodo, Phys. Rev. Lett. **67**, 3515 (1991).
[87] U. Fano, Phys. Rev. **72**, 26 (1947).
[88] J. A. Barmes and D. W. Allan, Proc. IEEE **54**, 176 (1996).
[89] A. Eke, P. Herman, L. Kocsis, and L. R. Kozak, Physiol. Meas. **23**, R1 (2002).
[90] J. W. Kantelhardt, S. A. Zschiegner, E. Koscielny-Bunde, S. Havlin, A. Bunde, and H. E. Stanley, Physica A **316**, 87 (2002).
[91] J. F. Muzy, E. Bacry, and A. Arneodo, Int. J. Bifurcation Chaos **4**, 245 (1994); A. Arneodo, E. Bacry, and J. F. Muzy, Physica A **213**, 232 (1995).
[92] H. E. Hurst, R. P. Black, and Y. M. Simaika Y M, *Long-Term Storage: An Experimental Study* (Constable, London, 1965).
[93] D. Prichard and J. Theiler, Phys. Rev. Lett. **73**, 951 (1994).
[94] P. Oświecimka, J. Kwapien, and S. Drozdz, Phys. Rev. E **74**, 016103 (2006).
[95] A. Linde and V. F. Mukhanov, Phys. Rev. D **56**, 535 (1997).
[96] I. Antoniadis, P. O. Mazur, and E. Mottola, e-print arXiv:astro-ph/9705200.
[97] P. J. E. Peebles, Astrophys. J. **510**, 531 (1999).
[98] P. J. E. Peebles, Astrophys. J. **510**, 523 (1999).
[99] M. S. Movahed and S. Khosravi, J. Cosmol. Astropart. Phys. **1103**, 012 (2011).
[100] J. L. Starck, N. Aghanim, and O. Forni, Astron. Astrophys. **416**, 9 (2004).
[101] H. Firouzjahi and S. H. H. Tye, J. Cosmol. Astropart. Phys. 03 (2005) 009.
[102] T. Fukushige, J. Makino, O. Nishimura, and T. Ebisuzaki, Publ. Astron. Soc. Jpn. **47**, 493 (1995).
[103] F. Bernardeau, Astron. Astrophys. **324**, 15 (1997).
[104] A. J. Banday, M. Górskik, C. L. Bennett, G. Hinshaw, A. Kogut, and G. F. Smoot, Astrophys. J. **468**, L85 (1996).
[105] M. Tegmark, Astrophys. J. **480**, L87 (1997).
[106] K. Schwarzschild, Vierteljahrsschrift Astron. Ges. **35**, 337 (1900).
[107] A. Einstein, Sitzungsber. Preuss. Akad. Wiss. 142 (1917).
[108] L. Perivolaropoulos, Phys. Rev. D **48**, 1530 (1993).
[109] A. Bershadskii, Phys. Lett. A **360**, 210 (2006).